[24] Rubesin, M. W., Pappas, C. C., and Okuno, A. F., "The effect of fluid injection on the compressible turbulent boundary layer—preliminary tests on transpiration cooling of a flat plate at $M = 2.7$ with air as the injected gas," NACA A55119 (1955).

[25] Green, L., Jr. and Duwez, P., "Fluid flow through porous metals," J. Appl. Mech. **18**, 39–45 (1951).

[26] Bartle, E. R. and Leadon, B. M., "Experimental evaluation of heat transfer with transpiration cooling in a turbulent boundary layer at $M = 3.2$," J. Aerospace Sci. **27**, 78–80 (1960).

[27] Bray, K. N. C., "Atomic recombination in a hypersonic wind-tunnel nozzle," J. Fluid Mech. **6**, 1–32 (1959).

[28] Widawsky, A., Oswalt, L. R., and Harp, J. L., "Experimental determination of the hydrogen recombination constant," ARS J. **32**, 1927–1929 (1962).

[29] Vanderslice, J. T., Weisman, S., Mason, E. A., and Fallon, R. J., "High-temperature transport properties of dissociating hydrogen," Phys. Fluids **5**, 155–164 (1962).

[30] Hoff, V. N., Gordon, S., and Morrell, V. E., "General method and thermodynamic tables for computation of equilibrium composition and temperature of chemical reactions," NACA 1037 (1951).

[31] "JANAF thermochemical data," Joint Army-Navy-Air Force Thermochemical Panel, Dow Chemical Co., Vol. 1 (1960)

[32] Irvine, T. F., Jr., Hartnett, J. P., and Eckert, E. R. G., "Solar collector surfaces with wavelength selective radiation characteristics," Solar Energy **2**, 12 (1958).

[33] Goulard, R. and Goulard, M., "One-dimensional energy transfer in radiant media," Intern. J. Heat Mass Transfer **1**, 81–91 (1960).

MAY-JUNE 1965 J. SPACECRAFT VOL. 2, NO. 3

A Radiation-Cooled Nuclear Rocket Nozzle for Long Firing Durations

SIDNEY ELKIND*
Arde-Portland, Inc., Paramus, N. J.

A thermal analysis was made of an uncooled nozzle for a 20-min firing. A 15,000-Mw reactor using 1000 psia hydrogen at 4500°R was considered. The analysis consisted of the determination of the transient temperature distribution within the proposed nozzle walls. Modes of heat transfer considered were gas convection, internal heat generation caused by gamma attenuation, conduction, and radiation to space. Design requirements were met by a shielded composite wall of tungsten, graphite, pyrolytic graphite, and René 41.

Nomenclature

c = specific heat
k = thermal conductivity
$\dot{q}$ = rate of volumetric heat generation within wall, Btu/hr-ft^3, at a point whose coordinate is x, at time θ
T = temperature
x = space coordinate, ft
α = thermal diffusivity
δ = wall thickness, ft
ϵ = wall emissivity
θ = time, hr
ρ = density
σ = 0.171×10^{-8} Btu/hr-ft^2-°R^4

Introduction

NUCLEAR rocket systems are currently being considered for many future space missions. In general, the missions are of long duration, requiring high-propulsion power levels. Reliability of all of the components is of paramount importance.

The nozzle not only must withstand the propellant-gas temperature and pressure, but it also must tolerate gamma heating during both operating periods and shutdown. A radiation-cooled nozzle is ideally suited for a nuclear rocket. Besides being inherently reliable, it also has the potential of simplifying the reactor-nozzle interface and making the nozzle independent of the balance of the system. The thermal analysis of a radiation-cooled nuclear nozzle presented in this paper is part of a feasibility study.[1] The specified design conditions include the following: power rating of 15,000 Mw, flow rate (H_2) of 800 lb/sec, inlet diameter of 6 ft, chamber pressure of 1000 psia, chamber temperature of 4500°R, exit-area ratio of 40:1, and "one firing."

The study is divided into two parts: 1) the determination of gamma heating within the wall and 2) the computation of the transient temperature distributions. Both the rate of gamma heating and the wall temperature distribution are functions of the wall configuration. An initial wall configuration was chosen, and transient temperature distributions were computed to determine its capability. The thermal design of the wall was changed, based on the results of this analysis, and the process was repeated until the design objective was achieved.

Heat Transfer

Material Considerations

The choice of materials for the component parts requires the matching of the respective properties and characteristics of proposed materials and the requirements of the parts. A basic consideration was that the materials selected and the design adopted could be fabricated, either at present or in the near future.

The requirements for an uncooled nuclear nozzle are similar to those for uncooled chemical rocket nozzles with the exception of the effects of gamma heating. Solid-propellant

Presented as Preprint 64-389 at the 1st AIAA Annual Meeting, Washington, D. C., June 29–July 2, 1964; revision received November 12, 1964. This paper presents one phase of a study carried out by Arde-Portland, Inc., for NASA Lewis Research Center under Contract No. NAS 3-3670. The author would like to express his appreciation to the Los Alamos Scientific Laboratory for making their QAD IV computer program available for the computation of gamma heating. Thanks are due to both NASA and Arde-Portland, Inc., for permission to publish this paper.

* Senior Heat-Transfer Engineer; now Engineering Specialist, Reaction Motors Division, Thiokol Chemical Corporation. Member AIAA.

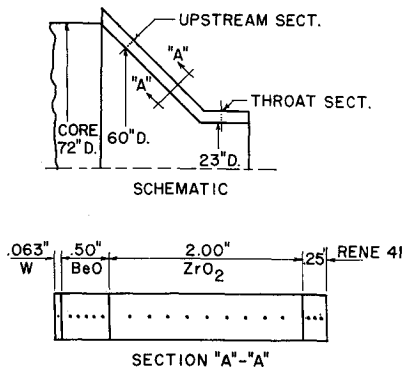

Fig. 1 Schematic section of the uncooled nuclear nozzle.

nozzles usually have a refractory liner in contact with the hot gas, an insulator to reduce the heat transferred through the wall, and an outer structural wall. The same general composite wall construction (Fig. 1) is postulated for the uncooled nuclear nozzle concept. The liner must be impervious to hot hydrogen and sufficiently ductile to transmit internal pressure loads to the insulation. Of the refractories, tungsten appears most attractive for this application. (Melting points of Cb and Mo are too close to the contemplated operating temperature; Ta is discounted because of its susceptibility to hydrogen embrittlement; and pyrolytic graphite, even though neither temperature-limited nor subject to embrittlement, would react chemically with the hot hydrogen to form hydrocarbon gases.)

The insulation material must have low thermal conductivity, stability at operating temperature, and adequate compressive strength to transmit the pressure load to the external structure. Promising materials include BeO, ZrO_2, and pyrolytic graphite. Other more exotic materials are available, but were not considered in the initial analysis. Pyrolytic graphite can be installed in several ways: 1) deposited in place, 2) laid up in the form of "molded" sections, and 3) wound on as cloth or foil. The method used will depend upon the nozzle design.

The structural wall must have strength at elevated temperatures and must also be able to tolerate a higher temperature in the soak condition. The nickel-base alloys look promising for this application. The 0.2% offset yield strengths of high-strength alloys that can be considered are listed in Table 1.

René 41 has been tentatively chosen for this component, primarily because of its excellent high-temperature strength coupled with ease of fabrication. Standards have been established for welding it.

Tungsten presents several problem areas in the fabrication of large component parts: 1) low-temperature brittleness and 2) welding difficulty. Greater ductility and hence easier fabrication is realized in alloys such as W-Re and W-Mo, without much sacrifice in either strength or melting temperature. Welded joints that are produced by conventional fusion processes result in highly embrittled weld zones that

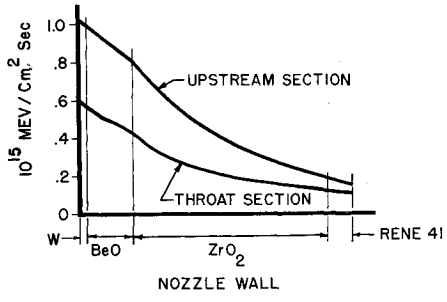

Fig. 2 Gamma flux distribution.

Table 1 Offset yield strengths of Ni-base alloys

Alloy	0.2% offset yield, psi	Temperature, °F
Rene 41	84,000	1600
Hastelloy "W"	22,000	1800
Rene 41	25,000	1800
Udimet 700	40,000	1800
In-100	52,000	1800

cannot sustain nominal stresses. Development effort to restore forged, extruded, or rolled properties in the crystallized weld zones is indicated.

Successful joints have been achieved by diffusion bonding using Ni-Pd interface cements. These joints are limited to a temperature of about 5000°F. Gas-pressure bonding has also been used for welding small sheets. Parameters of 10,000 psi, 2700°F, and 3-hr cycle time result in fairly coarse grain structures. The process is presently limited to diameters ≤ 5 in. Development effort is also being directed at raising recrystallization temperatures. Higher recrystallization temperatures imply longer operating times at higher temperatures before strength losses occur. This is of minor consideration in a design where the tungsten is not required to function as a structural member.

Method of Computing Nozzle Wall Temperature Distributions

The nuclear nozzle wall is subjected to Newtonian heating at the gas interface, conduction within the wall, internal heat generation caused by gamma attenuation, and radiation to space. The partial differential equation for the temperature for the one-dimensional case becomes

$$(\partial^2 T/\partial x^2) + (\dot{q}/k) = (1/\alpha)(\partial T/\partial \theta) \qquad (1)$$

where the wall material's thermal diffusivity $\alpha = k/\rho c$ is assumed to be constant.

If we consider a composite wall made up of three or more materials and apply the appropriate initial and boundary conditions, a closed-form solution is virtually impossible to obtain. An explicit finite-difference method of solution was therefore used.[2,3] In brief, it consists of dividing up the wall into an integral number of slabs and assuming that the slabs shrink to points or nodes. Each node is assigned the thermal properties and temperature of the volume it represents. A series of simple heat balances about each node is used to successively build up the wall temperature distribution as a function of time. The several nodal equations are of the form

$$T_n' = AT_{n-1} + BT_n + CT_{n+1} + D \qquad (2)$$

where T_n is the temperature of node n at time θ, and T_n' is the temperature of node n at time $\theta + \Delta\theta$. The coefficients A, B, and C operate on known temperatures at adjacent

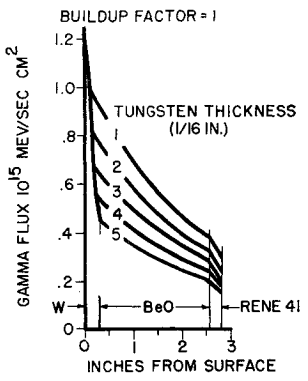

Fig. 3 Effect of tungsten thickness on gamma flux.

nodes to obtain the temperature at node n at a future times Since physical considerations require that the coefficients do not become negative, this becomes the basis for a stable solution.

Heating Rates within Nozzle Walls

In a nuclear rocket nozzle, gamma radiation leads to internal generation of heat, which is essentially independent of the temperature level of the working fluid; the wall temperature can rise above that of the gas. The Los Alamos Scientific Laboratory's QAD IV computer program was used to determine the gamma flux distribution within the wall[4,5]; this 7090 computer program calculates gamma radiation from a distributed source (in our case, the reactor) through attenuating materials, the boundaries of which can be described by quadratic surfaces. A distributed source is divided into a number of point-isotropic sources of discrete energy groups and is normalized to give the desired total power. The program determines the line-of-sight distances through each attenuating material from a source point to a detector point; it then uses exponential attenuation (with energy-dependent mass attenuation coefficients) and a single build-up factor. This process is continued for each source point and for all of the energy groups; finally, these contributions are summed for each detector point.

The axial distribution of gamma flux (for the wall of Fig. 1) is shown in Fig. 2, and the flux through the wall is given in Fig. 3 (for a build-up factor of 1). The latter is reduced by a factor of 3 (inside to the outside) because of attenuation by the intervening material. The throat values are approximately half as large as those upstream because of the greater distance from the core and the shielding supplied by the convergent section. The effect of using the larger build-up factor of aluminum, which is equivalent to that of the core material, is evident from Fig. 4; the flux values are 3 times as high as in Fig. 3. Increasing the thickness of the W liner from $\frac{1}{16}$ to $\frac{5}{16}$ in. cuts the flux in half.

The gamma heating rates in a wall with a $\frac{9}{16}$-in.-thick W liner are presented in Fig. 5. The discontinuities in the curves result from the method of weighing the material nuclear properties. The volumetric rate of heat generation varies from 3×10^7 Btu/hr-ft^3 in the tungsten at the upstream section to 1×10^6 in the René 41. These rates will significantly affect the transient temperature distribution in the nozzle wall.

Tolerable Gamma Heating: Approximate Analysis

The heat generation within the nozzle wall caused by gamma heating can nullify the effect of the insulation. The structural part of the wall can be raised above design temperature, even though conduction through the wall is reduced. In order to determine the order of magnitude of gamma heat generation that can be tolerated by the René 41, an approximate analysis was made.

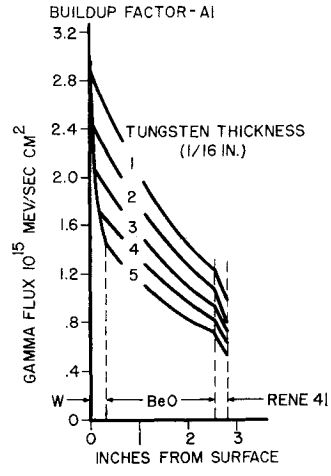

Fig. 4 Effect of tungsten thickness on gamma flux.

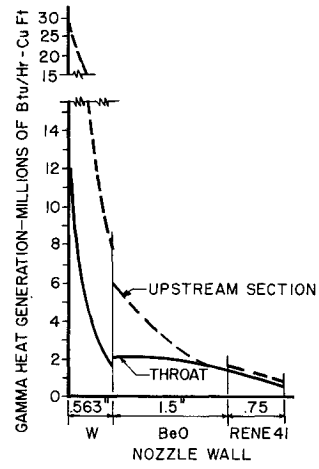

Fig. 5 Gamma heat generation.

Consider the thermal insulation to be perfect and perform a steady-state heat balance on the René 41. It is heated by internal heat generation

$$q_{gen} = \dot{q}\delta A$$

and cooled by radiation to space

$$q_{rad} = \sigma \epsilon A T_w^4$$

The steady-state temperature T_w (assuming a flat temperature profile) is

$$T_w = (\dot{q}\delta/\sigma\epsilon)^{0.25}$$

The wall temperature has been plotted in Fig. 6 for variations in heat generation rate and wall thickness. For a design limit of 2260°R, the maximum heat generation rate is limited between 0.25×10^6 and 0.5×10^6 Btu/hr-ft^3. However, the results of the QAD program (Fig. 5) show that the gamma heating rate is greater than 1×10^6 Btu/hr-ft^3. Thus gamma heating is seen as a potential problem area. It can be reduced by shielding, separation, or reduction of the source-power density. Shielding can be accomplished by increasing the W thickness and by using auxiliary W shields within the gas stream. (The effect of thicker W layers is presented later.) To obtain a significant gamma reduction caused by separation, great distances must be involved; since the available distance is limited, this approach is not practical in the present application. The source-power density can be reduced by keeping the core size constant, but reducing the power output; the gamma heating rate will decrease in direct proportion. (The effect on T_w distribution is covered later.)

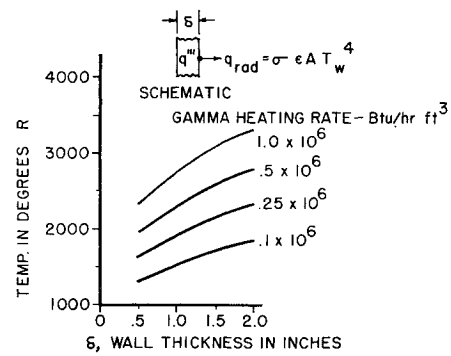

Fig. 6 Steady-state temperature of a heat-generating wall radiating to space.

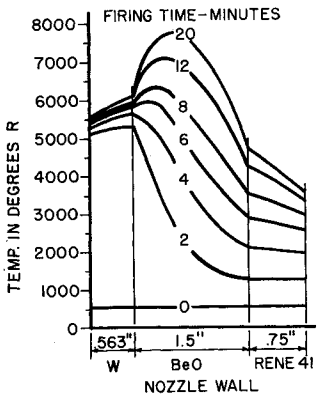

Fig. 7 Transient temperatures (upstream section).

Transient Wall Temperature Distribution

Transient temperatures were computed within the wall at two sections: 1) upstream where the gas coefficient is low and 2) at the throat where the highest coefficient exists. The convection coefficients, computed by means of the Bartz equation,[6] at the throat and upsteam at an area ratio of 6.8, are, respectively

$$h_g^* = 4950 \text{ Btu/hr-ft}^2\text{-°R}$$

$$h_g = 830 \text{ Btu/hr-ft}^2\text{-°R}$$

In the quest for a wall that could tolerate a 20-min firing, the thickness of the materials was varied, and the material arrangement was modified on the basis of the resulting gamma flux and temperature distribution. The initial runs showed that a thin W liner does not reduce the gamma heating rate significantly; the effect in the René 41 structure can be seen in Fig. 4. On this basis, a liner $\frac{9}{16}$ in. thick was chosen. It is visualized as made up of thin layers to reduce thermal shock. Only the initial layer need be gas tight.

The temperature distribution in the upstream section for the wall initially proposed, with the tungsten thickness increased to $\frac{9}{16}$ in., is shown in Fig. 7. The temperature limits of BeO and René 41 are exceeded in 2 and 4 min, respectively. In the first 2 min, the liner temperature is already above that of the gas; at this time, the highest temperature is at the W interface, and the René 41 is at a uniform temperature. As the firing continues, a peak develops within the BeO insulation, and a noticeable slope appears in the René 41 structure. The peak is attributed to the fact that heat is generated by gamma rays within the material faster than it can be extracted by radiation at the rear surface and convection at the inner surface. As the insulation is made thicker, the thermal resistance to either surface increases and the peak becomes higher. The temperature gradient in the René 41 reaches 1000°R/in. in 12 min.

The corresponding temperature distributions in the throat section were found to be similar; the René 41 limit was exceeded in 5 min, and the BeO became marginal late in the firing. The temperature peak within the insulation appeared later than it did in the upstream section.

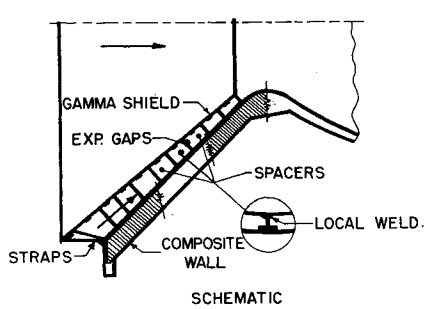

Fig. 8 Internal gamma shield concept.

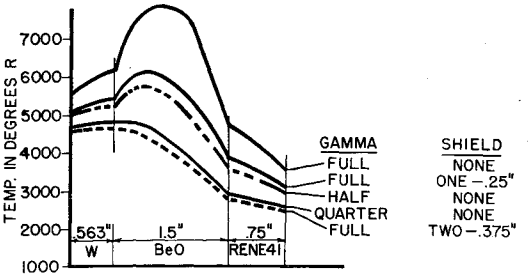

Fig. 9 The effects of shielding and gamma reduction on the wall temperature distribution after a 20-min firing.

Effects of Reduced Gamma Heating

In order to see the effects of reduced heat generation, the computed gamma was arbitrarily reduced by factors of 2, 4, and 10. Gamma reduction may be attained (in proportion) by reducing the total power of the core but keeping its dimensions constant. The results for the upstream section showed that the temperature peak within the insulation decreases as the heat generation rate is decreased, virtually disappearing at the $\frac{1}{4}$ rate, at which rate the wall would last 9 min. At the $\frac{1}{10}$ rate, it would last 16 min. Results at the throat section were similar.

Another way to reduce the gamma heating rate is to shield the wall from the reactor core. This must be done with a minimum interference to the core gas flow. This concept is shown in Fig. 8. The tungsten shield is retained by supports at the upstream end. It is kept concentric with the wall by longitudinal spacers. This arrangement is similar to that of the cooling liner in ramjet engines. This method of shielding is potentially attractive, since the shield is totally surrounded by the gas. Thus, its temperature will not rise significantly above that of the gas whereas, if its thickness were added to the W liner, the resulting total thermal resistance could be high enough so that the tungsten design temperature could be exceeded at the insulation interface.

The effect of both single and double liners of various thicknesses is presented in Fig. 9. The effect of reduced gamma flux is also indicated. A single $\frac{1}{4}$-in. shield is approximately equivalent to the $\frac{1}{2}$ flux level, and two $\frac{3}{8}$-in. shields reduce the temperatures about the same as a reduction to the $\frac{1}{4}$ flux level. A single shield of greater thickness can reduce the temperature as effectively as multiple shields in which the combined thickness is equal to that of the single shield. Moreover, supporting a shield operating at high temperature within a nozzle is difficult, and the difficulty increases as the number of shields increases, so that a single, thicker shield is probably more desirable.

The wall construction was changed with pyrolytic graphite replacing the BeO to take advantage of its higher temperature capability. The most promising combination also had a layer of tungsten within the wall. With full gamma flux, this wall can withstand a 6-min firing, the critical material being the graphite. The René 41 remains below its design

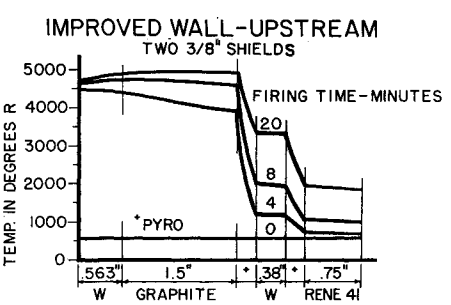

Fig. 10 Transient temperature distributions.

Table 2 Heat balance for improved wall after 14 min at $\frac{1}{2}$ gamma flux level

Mode of heat transfer	Btu	% of g_{gen}
Gamma heating in wall	297,000	100
Convection to core gas	196,400	66
Radiation to space	5,800	2
Stored in wall	94,800	32

point for 8 min. At the $\frac{1}{4}$ gamma flux level, this wall can withstand the desired 20-min firing. Such a reduction can be attained by using either two $\frac{3}{8}$-in. or one $\frac{3}{4}$-in. shield.

The temperature distribution in the upstream section of the shielded wall is shown in Fig. 10. The structural wall temperature is below 1600°F. Results for the throat section were almost identical. The temperature profiles within the W and the René 41 are flat, indicating that thermal stresses will be low. This configuration can withstand the 20-min firing with a margin for temperature rise during soak.

A heat balance (Table 2) was made on the upstream section of this wall to determine the relative magnitudes of the heat-transfer modes involved. The $\frac{1}{2}$ gamma flux level was considered after 14 min of firing. The balance included internal heat generation by gamma heating, heat transfer from the wall to the core gas, heat storage within the wall, and radiation to space.

It is evident from Table 2 that the gamma heating accounts for all of the heat transferred and that the more effective cooling method is convection to the gas stream. Although radiation to space is a numerically small quantity, it is sufficient to maintain the structural shell below its design temperature.

Effect of Gas Temperature and Pressure Reductions

Runs were made with gamma flux with the gas temperature reduced to 4000° and 3500°R; the internal peak temperature was reduced slightly, but the structural shell was unaffected. Runs were also made with the gas pressure reduced to 750 and 500 psia. In order to maintain the thrust constant, an increase in throat diameter is required. The gas convection coefficient is, therefore, reduced by the 0.9 power of the pressure ratio. Again, the effects were only felt near the gas-side surface. The René 41 was not affected.

Temperature Distribution in a Solid Tungsten Wall

Steady-state temperature achieved in a solid W wall within several minutes of firing is shown in Fig. 11. The upstream section has a temperature peak that increases from 4700° to 5500°R as the wall is varied from 0.75 to 3 in. This effect is caused by gamma heating and the increased thermal resistance from the interior to both surfaces where cooling is attained. Although the higher convective coefficient at the throat is sufficient to depress the peak, the strength of W at the temperature attained is not high enough to make the 4-in. wall structurally sound. The large temperature gradients are noteworthy; the resulting thermal stresses could not be tolerated. Thus, the shielded, radiation-cooled wall uses the tungsten more effectively than it can be used as a solid wall.

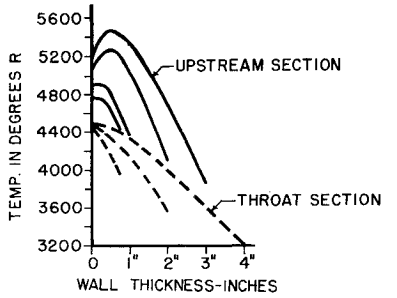

Fig. 11 Steady-state temperatures in a solid tungsten wall.

Conclusions

An uncooled, nuclear nozzle wall shielded by two $\frac{3}{8}$-in. tungsten shells is feasible, from a temperature standpoint, for a 20-min firing. The shields effectively reduce the gamma flux by a factor of 4. The primary problem area in long firing duration capability is gamma heating, which can be reduced by shielding the nozzle wall or by reducing the reactor core-power density. One $\frac{3}{8}$-in. W shield has the same effect as halving the core-power density; two $\frac{3}{8}$-in. shields are equivalent to reducing the power density to $\frac{1}{4}$.

Effective thermal insulation is required to insulate the outer structural shell from the internal core gas. The combined effects of this insulation and gamma heating result in a hot-side wall temperature above that of the gas. The gas therefore cools the wall. For these shielded walls, the structural shell temperature depends directly upon gamma heating and is not affected by either core gas temperature or pressure reduction.

This study has concentrated on feasibility from a temperature standpoint. Potential fabrication problem areas have been identified (e.g., supporting the internal shields and making the large gas-tight tungsten liner). More detailed investigations and development are required to establish over-all feasibility.

References

[1] Elkind, S., "Nuclear rocket engine nozzle study," NASA Rept. CR-54000 (1964).

[2] Dusinberre, G. M., *Heat Transfer Calculations by Finite Differences* (International Textbook Co., Scranton, Pa., 1961), Chap. II.

[3] Schneider, P. J., *Conduction Heat Transfer* (Addison-Wesley Publishing Co., Inc., Cambridge, Mass., 1955), Chap. XII.

[4] Malenfant, R. E., private communication, Los Alamos Scientific Lab., Los Alamos, N. Mex. (July 1963).

[5] Blizard, E. P., "Nuclear radiation shielding," *Nuclear Engineering Handbook*, edited by H. Etherington (McGraw-Hill Book Co., Inc., New York, 1958), Sec. 7-3.

[6] Bartz, D. R., "A simple equation for rapid estimation of rocket nozzle convective heat transfer coefficients," Jet Propulsion **27**, 49–51 (1957).